*Sensors and Materials*, Vol. 10, No. 8 (1998) 487–501
MYU Tokyo

S & M 0348

# A New Type of Vibration Sensor Using an Optical Fiber with a Bulb-Lens as a Cantilever

Katsuhisa Toshima and Mitsuteru Kimura*

Electrical Eng., Faculty of Eng., Tohoku-Gakuin University
1-13 Chuo-1, Tagajo, Miyagi 985-8537, Japan

(Received January 5, 1998; accepted Jyly 9, 1998)

***Key words***: optical-fiber sensor, vibration sensor, bulb-lens, cantilever, micromachining

A new design of the bulb-ended fiber lens used for emitted-light collimation and a vibration sensor comprising an optical-fiber cantilever with the bulb-lens, fabricated using the silicon micro-fabrication technique, are proposed and demonstrated. Nearly flat frequency dependence of the optical output is observed in the 40–1200 Hz frequency range under constant acceleration. Acceleration resolutions of 0.3 and 1.0 m/s$^2$ are attained in the transmission-type and the reflection-type devices, respectively. Vibration with many modes from a vibrator undergo fast Fourier transform (FFT) analysis of optical signals obtained from these vibration sensors.

## 1. Introduction

Recently, numerous studies on optical-fiber sensors for measuring physical quantities have been reported. An optical-fiber vibration sensor is promising for sensing unusual vibrations in special equipment or environments such as high-voltage transformers or cars, because of its insensivity to high electromagnetic fields compared to vibration sensors based on capacitive[1] or piezoelectric[2] working principles.

Conventional optical-fiber vibration sensors, which use a Si beam as an optical-shutter[3] and a base of the optical-waveguide,[4–6] are not very sensitive to vibration because of no seismic mass.[3,6] Moreover, optical alignment and coupling between the optical fiber and the waveguide have been difficult in these sensors.[4–6]

*Correspondence author

An optical-fiber accelerometer, which is composed of a glass plate cantilever bonded on the glass substrate, and a GRIN-lens bonded with an optical fiber have been reported.[7] However, this accelerometer is difficult to fabricate because of the need for manual bonding of two glass plates and manual optical alignment.

A usual bulb-lens formed by merely melting the end of the fiber has essentially been unable to collimate the output light beam.[8,9]

Therefore, to realize a simple, low-cost vibration sensor, we developed a new type of vibration sensor having an optical fiber that uses a bulb-lens as a cantilever set in a V-groove on a silicon substrate. A new type of bulb-lens, which emits a nearly collimated light beam and also acts as the seismic mass of the vibrational optical-fiber cantilever, is used in this vibration sensor. In this paper, a new design of the bulb-ended fiber lens (bulb-lens) is proposed and demonstrated according to the formula deduced theoretically, and a new type of vibration sensor, i.e., an optical-fiber vibration sensor combined with an optical-fiber cantilever with a bulb-lens and the silicon micromachining technique, is also proposed and demonstrated.

## 2. Principle and Structure of the Optical-Fiber Vibration Sensor

Figure 1 shows the structure of a new type of optical-fiber vibration sensor using the optical fiber with a bulb-lens for vibration. Our optical-fiber vibration sensor developed has two types: transmission-type and reflection-type. The light emitted from the bulb-lens is coupled into the optical fiber in the transmission-type sensor, while the emitted light is

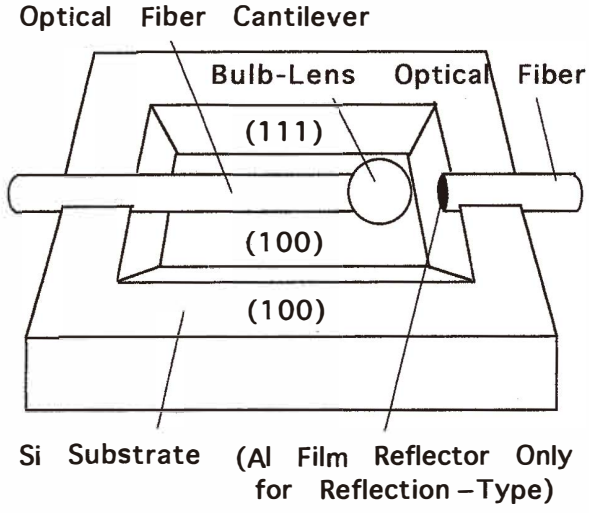


Fig. 1. Structure of the optical-fiber vibration sensor.

reflected at the reflector of the Al thin film and recoupled into the bulb-lens in the reflection-type sensor. When the sensor is vibrated, the optical intensity received at the optical fiber or at the recoupled bulb-lens change.

This optical-fiber cantilever with the bulb-lens is set in one V-groove and the optical fiber is in the other V-groove formed by anisotropic etching on the surface of the Si (100) substrate. Setting the fiber in the V-groove enables self-alignment of the two fibers. Evaporated Al thin film is deposited as a reflector on the cut surface of the optical fiber in the reflection-type vibration sensor, while there is no reflector of the Al film in the transmission-type sensor. In these sensors, the optical-fiber cantilever with the bulb-lens and the optical fiber are sandwiched by two symmetrical Si substrates with V-grooves.

## 3. Model of a Bulb-Lens as an Optical Collimator Lens

In Fig. 2, a model of the new optical-fiber bulb-lens is shown, where point A is the end of the fiber core, O the center of the spherical end formed using a coreless optical fiber, $R$ the radius of the bulb-lens and $L$ the distance between the end of the core and the top of the bulb lens.

We assume that the guided light beam will disperse at the end of the core when it is spliced with coreless fiber, and the end point of the core, A, will act as a light source. Let $n_1$ and $n_2$ be the refractive indices of the bulb-lens and air, respectively, and $\theta_1$ and $\theta_2$ correspond to the refractive angles at point D on the surface of the bulb-lens.

We have found the condition, $L = 3R$, can be deduced from the Abbe invariant formula of the lens for a near axis ray[10] as:

$$n_1 (1/R - 1/L) = n_2 (1/R - 1/L'). \quad (1)$$

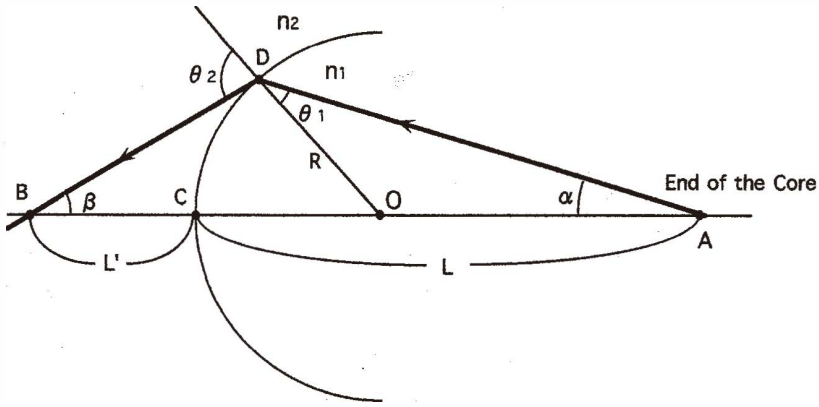


Fig. 2. Model of a bulb-lens for emitted light collimation.

For $L' = -\infty$,

$$L = n_1 R \ / (n_1 - n_2). \tag{2}$$

For $n_1 = 1.5$ and $n_2 = 1$, we get the following relation,

$$L = 3R. \tag{3}$$

We can expand eq. (3) for arbitrary media of refractive indices, $n_1$ and $n_2$, as a condition for collimation of the emitting beam. Putting $X = n_1/n_2$ and $Y = L/R$, a simple formula is deduced as,

$$Y - 1 = 1 \ / (X - 1). \tag{4}$$

In Fig. 3, the $X$–$Y$ relation in eq. (4) is shown. In this figure, we can see the collimating condition of the bulb-lens in arbitrary media, such as the quartz bulb-lens in water.

## 4. Formation of the Bulb-Lens

Our optical-fiber bulb-lens is formed as follows. A single-mode silica fiber 125 $\mu$m in diameter (10 $\mu$m or 50 $\mu$m core) is spliced with a coreless fiber with the same diameter

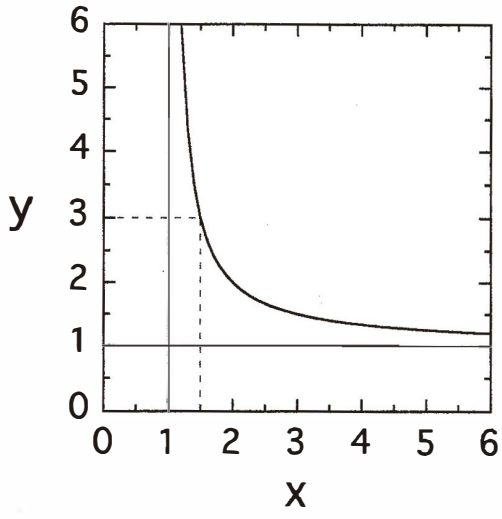


Fig. 3. Relation between $X = n_1/n_2$ and $Y = L/R$.

using arc-discharge splicing equipment. Then, the spliced coreless fiber is cut with a cutting tool so that the calculated length of the coreless fiber is that which takes into account that after the arc-discharge melt which satisfied $L = 3R$, the volume of the bulb-lens remains.

Distributions along the $y$-axis and the $x$-axis of the output beam from the formed bulb-lens with the 10 $\mu$m core are measured using the optical fiber as shown in Fig. 4. The half-width $\Delta\Phi$ of the output distribution along the $y$-axis for originally cut length $L_0$ of the 922 $\mu$m coreless fiber was about 30 $\mu$m, as shown in Fig. 5(a). Output power measurement is carried out using the optical power meter for optical-fiber attenuation-measurement with a LED light with a 1.3 mm wavelength. A collimating length of about 1.6 mm is obtained as shown in Fig. 5(b), but in the case of the 50 $\mu$m core, it was slightly shorter than that obtained in the case of 10 $\mu$m.

## 5. Evaluation of the Optical-Fiber Vibration

Experimental setups for vibration sensing in the transmission-type and the reflection-type sensors are shown in Figs. 6(a) and 6(b), respectively. A loudspeaker is used as a vibrator. Light wavelength $\lambda$ = 834 nm from a laser diode is fed into the optical-fiber cantilever with the bulb-lens, and is then coupled into the optical fiber in the transmission-type sensor or is recoupled into the bulb-lens in the reflection-type sensor. Optical signals corresponding to the vibration are received at the optical fiber or at the recoupled optical-fiber cantilever, propagate through it, and are then detected by a photodiode.

The Michelson-interferometer system is used to measure the vibrational acceleration. The quantity of the vibrational acceleration is calculated by the maximum velocity $v_{max}$ of the cone of the loudspeaker. Maximum velocity $v_{max}$ is also calculated by the maximum frequency $f_{max}$ obtained by FFT analysis of the optical output of the Michelson-interferometer system. $v_{max}$ is given by the following:

$$v_{max} = \frac{\lambda f_{max}}{2}. \tag{5}$$

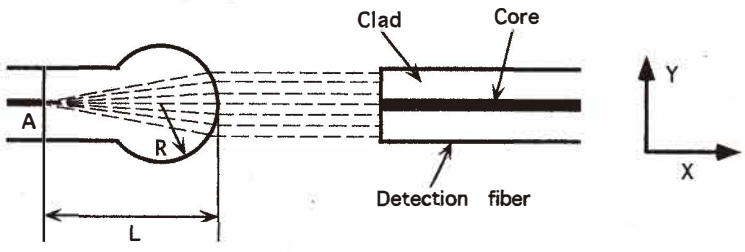


Fig. 4. Measurement of distribution of the output beam emitted from the bulb-lens.

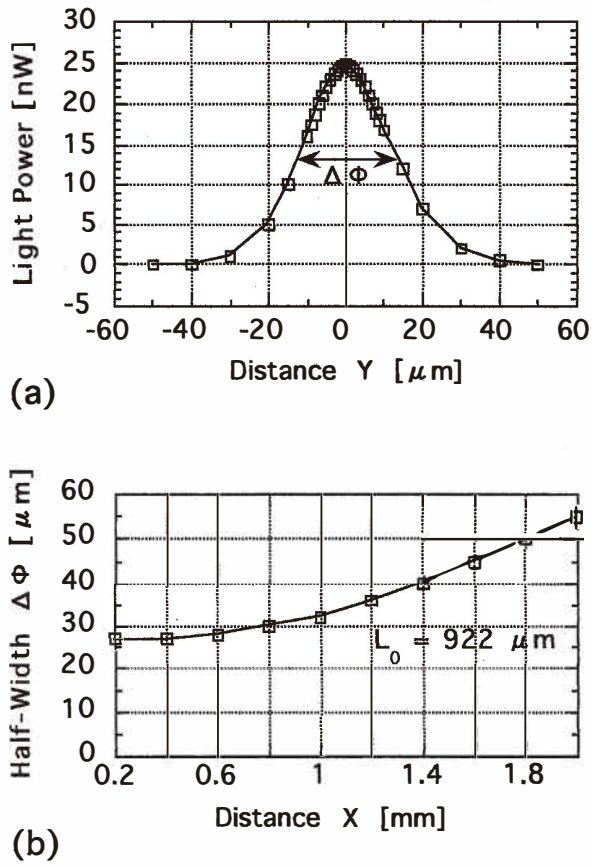


Fig. 5. Half-width $\Delta\Phi$ of the output distribution along the $y$-axis (a), and change in $\Delta\Phi$ along the $x$-axis (b).

A He-Ne laser ($\lambda = 632.8$ nm) is used as a light source in our Michelson-interferometer system. Maximum acceleration $a_{max}$ is deduced from the following equations:

$$y = \mathrm{A} \sin \omega t, \tag{6}$$

$$y = \frac{dy}{dt} = A\omega \cos \omega t, \quad v_{max} = A\omega, \tag{7}$$

$$a = \frac{d^2y}{dt^2} = -A\omega^2 \sin \omega t, \tag{8}$$

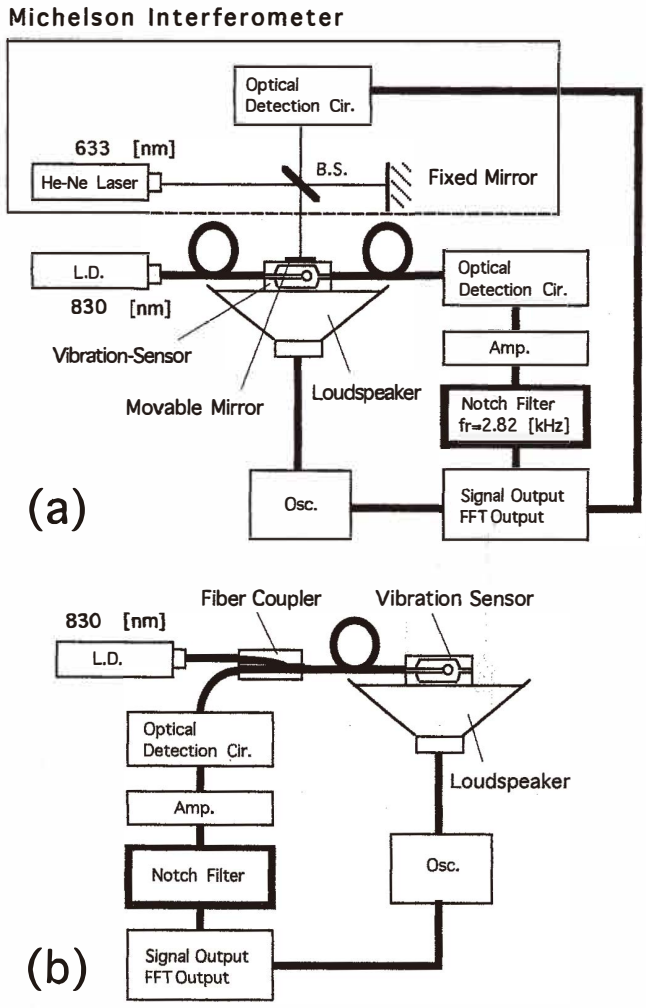


Fig. 6. Experimental setups for vibration sensing. (a) Transmission-type, (b) reflection-type.

$$a_{\max} = A\omega^2 = v_{\max}\,\omega, \tag{9}$$

where $y$ is the amplitude of the cone of the loudspeaker, $A$ its maximum amplitude and $\omega$, the excitation angular frequency.

We can see from eq. (9) that the quantity of excitation frequency $f$ multiplied by the maximum velocity $v_{\max}$ of the vibrator (the loudspeaker) is proportional to the maximum

acceleration $a_{max}$. In our experiments, the voltage applied to the loudspeaker is controlled so as to provide constant acceleration for this optical vibration sensor. So, for example, a sinusoidal voltage applied to the loudspeaker at the resonance-frequency of the loudspeaker attached by the sensor is set to be smaller than that at nonresonant frequency in order to provide constant acceleration.

## 6. Simulations for Resonance-Frequency of the Optical Fiber with the Bulb-Lens

We have calculated the resonance-frequency *fr* for the optical-fiber vibration sensor as a cantilever of the fiber with the bulb-lens as a weight shown in Fig. 7. In this system, the resonance-frequency *fr* is given by

$$fr = \frac{1}{2\pi l^2}\sqrt{\frac{3.044EI}{(0.227+\mu)\rho S}}, \tag{10}$$

$$\mu = \frac{m}{\rho S l}, \tag{11}$$

where $EI$ is the stiffness of the fiber, $l$, the length of the fiber, $\rho$, the density, $S$, the cross section of the fiber and $m$, the bulb mass.

In Fig. 8, calculated results of the resonance-frequency *fr* as a function of the ratio of the bulb radius $R$ to the fiber radius $r$, $R/r$, for various values of fiber length $l$ are shown, where $R$ and $r$ are related to $m$ and $S$, respectively, and are reflected in the resonance-frequency *fr*, through $\mu$, in eq. (11). The calculated curve and experimental data for *fr* are shown in Fig. 9. We can see the calculated curve agrees well with experimental one.

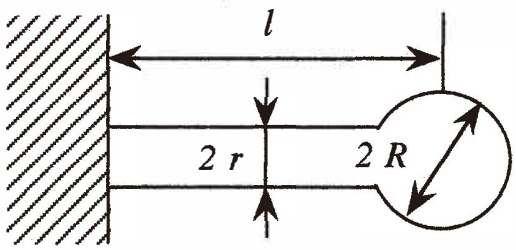


Fig. 7. Model for vibration of the optical-fiber cantilever with a bulb-lens.

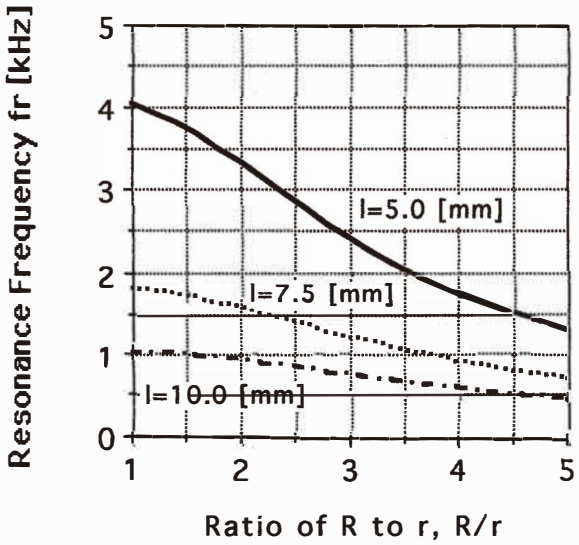


Fig. 8. Calculations for the ratio of the bulb radius $R$ to the fiber radius $r$, $R/r$, dependence of the resonance frequency $fr$ for fiber lengths $l$.

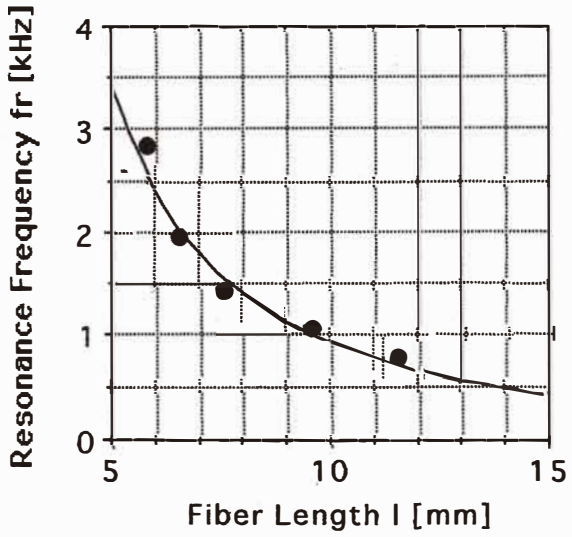


Fig. 9. Fiber length $l$ dependence on the resonance frequency $fr$ (solid line: theoretical; dots: experimental.).

## 7. Results

### 7.1 *Elimination of resonance-frequency component*

The optical output of the transmission-type sensor plotted against the excitation frequency *f* by the loudspeaker is shown in Fig. 10. We can see a large peak at the 2.8 kHz resonance-frequency *fr* of the optical fiber with the bulb-lens, and we can also find some peaks (dotted line in the figure) which correspond to frequencies obtained by dividing the resonance-frequency *fr* by an integer *n* (i.e., *fr/n*). We know that the frequency of *fr/n* (for example, *fr/n* = 1.4 kHz and 940 Hz for *n* = 2 and 3, respectively) can excite the *fr* component. So we observe the optical output signal of the *fr* frequency at the *fr/n* frequencies. We used a notch-filter with a dip at *fr* to eliminate the *fr* component in the electrical output signal. Peaks at *fr/n* disappeared in the characteristics with a notch-filter (solid line) as shown in Fig. 10, unlike that without the notch-filter (dotted line). However, peaks near *fr* still remained. This may be due to nonlinear effects caused by large vibration of the bulb-fiber. In Fig. 10 other peaks are also found, and may originate from vibrational modes in the loudspeaker.

The optical output at 940 Hz, which corresponds to *fr*/3, is shown in Fig. 11. Figure 11(a) shows the waveforms of the output signal without the *fr* notch-filter, and we can see that a frequency component measuring three times the excitation frequency *f* of 940 Hz, namely the resonance-frequency *fr*, exists in the output waveform. Figure 11(b) shows that with a notch-filter, we only find a frequency component equal to the excitation frequency *f*. Relatively large initial displacement (about 30 $\mu$m) of the optical axes between two fibers and small vibrational amplitude of the optical-fiber cantilever lead to equal frequency components between the excitation and vibration frequencies.

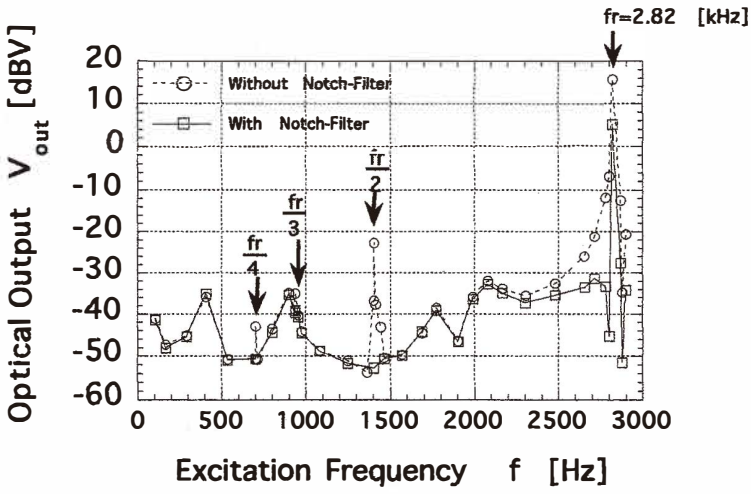


Fig. 10. Frequency dependence of the optical-fiber vibration sensor driven by a loudspeaker.

(a)

(b)

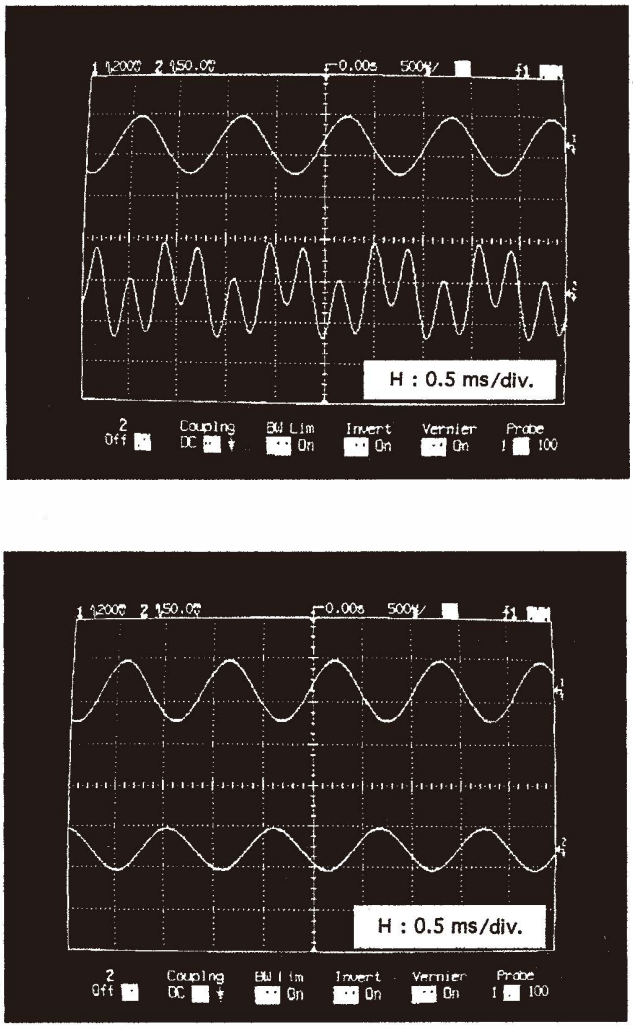


Fig. 11. Optical output signals at an excitation frequency of 940 Hz ($fr/3$) without notch-filter (a) and with notch-filter (b). Top and bottom signals in both figures correspond to the excitation signal [200 mV/div.] and the output signal [50 mV/div.], respectively.

## 7.2 *Frequency dependence of optical output under constant acceleration*

In Fig. 12, optical output of the vibration sensor is plotted against the excitation frequency $f$, which is measured under constant acceleration as a parameter. Scatter in the data plots in Fig. 12 may be due mainly to poor control of the voltage amplitude of

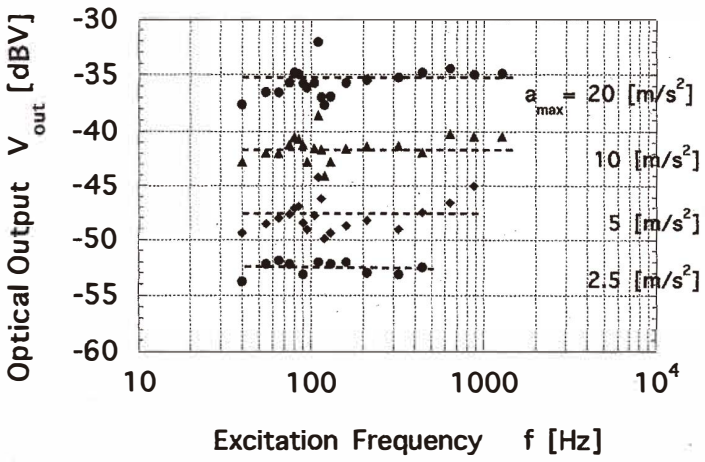


Fig. 12. Optical outputs of the vibration sensor plotted against the excitation frequency $f$ under the constant acceleration of 20, 10, 5 and 2.5 m/s$^2$.

excitation frequencies applied to the loudspeaker to maintain constant acceleration. From Fig. 12, we can see that our optical vibration sensor has a nearly flat frequency dependence in the observed frequency range of 40–1200 Hz, and that the output signal is almost proportional to the acceleration values.

### 7.3 *Dependence of acceleration in optical output*

Figure 13 shows the acceleration dependence of optical output for both the transmission-type and the reflection-type vibration sensors. The sensor we developed has high acceleration resolutions (SNR = 1) of 0.3 and 1.0 m/s$^2$ for the transmission-type and the reflection-type, respectively. Actual sensor acceleration is calibrated by the Michelson-interferometer. It is found that the sensitivity of the reflection-type sensor is less than one third that of the transmission-type sensor, and their optical outputs are nearly proportional to the acceleration, $a$, in the observed acceleration range of 0.5–20 m/s$^2$.

The vibrational amplitude at the end of the optical fiber (at the bulb-lens) is estimated to be between 1 and 2 $\mu$m by comparing the experimental light-intensity change (both dc and ac components) caused by vibration with the theoretical one which uses the optical coupling model under an excitation frequency of 1 kHz and acceleration of 10 m/s$^2$.

### 7.4 *FFT vibration analysis*

Figures 14(a) and 14(b) show the optical output signal and its FFT signal, respectively, when the sensor attached to the loudspeaker used as a vibrator is excited by three different mixed frequencies of 1.25, 1.66 and 2.23 kHz. We observe three peaks in the FFT spectrum corresponding to the excitation frequencies. We could ascertain reproducible FFT analyses for many kinds of vibrators. The height of the peak in the FFT spectrum will

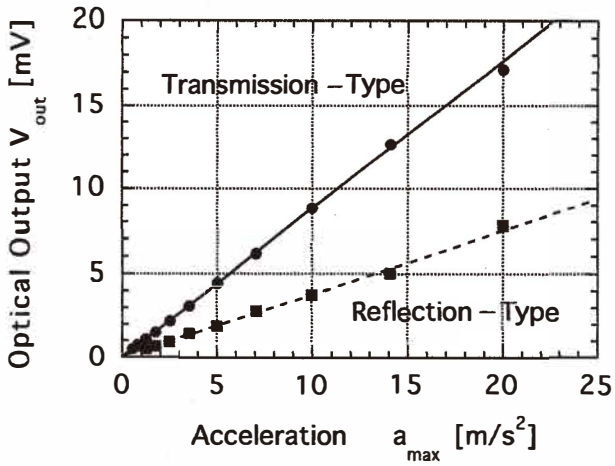


Fig. 13. Acceleration, $a$, dependence of optical outputs, $v_{out}$, for the transmission-type and the reflection-type sensors.

be proportional to the acceleration, $a$, of the vibration of the frequency component because the vibrational amplitude of the input fiber used as a cantilever is much smaller than the relatively large initial displacement (about 30 $\mu$m) of the optical axes between two fibers. Since the sensor is covered with a silicon plate, we can neglect the effect of ambient light in the FFT analysis.

## 8. Conclusions

A new design of the bulb-lens formed at the end of an optical fiber for emitted-light collimation is proposed and demonstrated, and the bulb-lens optical fiber is applied to a new type of vibration sensor fabricated by Si micromachining technologies. A reflection-type vibration sensor which uses only one optical fiber without the optical fiber for light transmission as well as a transmission-type vibration sensor have been developed.

A nearly flat frequency dependence of the output signal was obtained in the observed frequency range of 40–1200 Hz under constant acceleration. Acceleration resolution values (or the noise level) of 0.3 and 1.0 m/s$^2$ for the transmission-type and the reflection-type vibration sensors, respectively, are attained in our experiments. Acceleration resolution can be increased by increasing the length of the optical-fiber cantilever if the highest observable frequency is allowed to be lower. FFT analysis of optical signals from the vibration sensors confirmed occurrence of vibration in various modes. These vibration sensors can be applied to acceleration sensors.

The optical-fiber vibration sensor developed is advantageous because of its simple structure and low-cost fabrication since mass production of the V-groove by Si

(a)

(b)

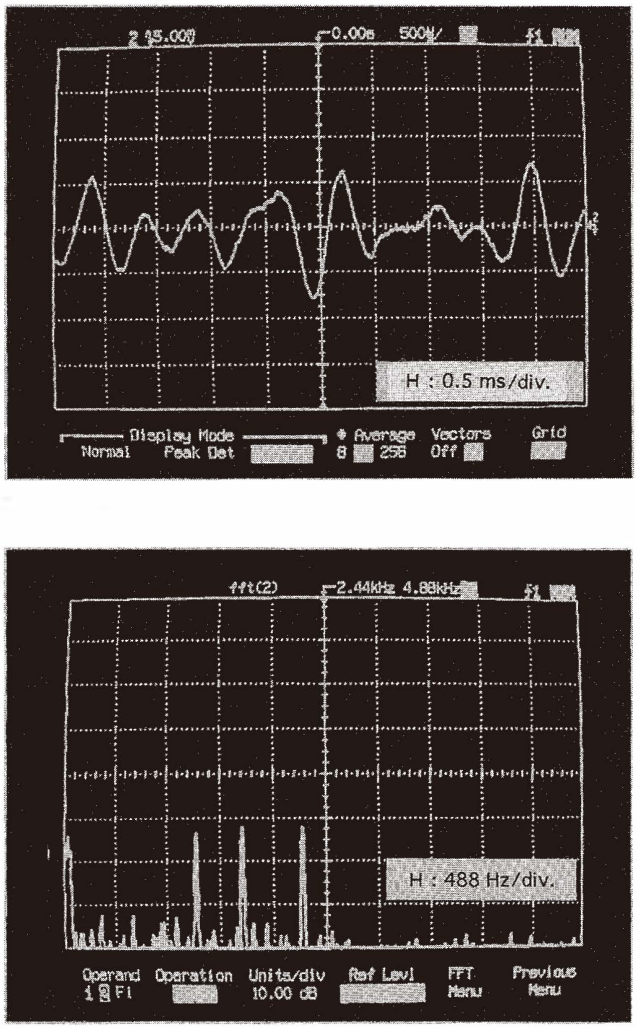


Fig. 14. Optical output signal [5 mV/div.] (a) and its FFT signal [10 dBV/div.] (b) from the vibration sensor excited by mixed three different frequencies of 1.25, 1.66 and 2.23 kHz.

micromachining sets the optical fiber and eases optical alignment. The reflection-type vibration sensor is more useful for actual vibration sensing than the transmission-type because it requires only one optical fiber for light transmission.

## Acknowledgments

The authors wish to thank Mr. T. Suzuki for his assistance in experiments.

## References

1 T. Sasayama, S. Suzuki, S. Tsuchitani, A. Koide, M. Suzuki, T. Nakazawa and N. Ichikawa: Sensors and Actuators A **54** (1996) 714.
2 K. Okada: Proc. 8th Int. Conf. Solid-State Sensors and Actuators (Transducers '95) / Eurosensors IX (Sweden, 1995) p. 566.
3 D. Scholz, E. Peiner, A. Schlachetzki, H. Fritsch, R. Mikuta and P. Hauptmann: Proc. OPTO 96 (1996) p. 291.
4 E. Ollier, P. Labeye and P. Mottier: Electron. Lett. **33** (1997) 525.
5 T. Storgaard-Larsen, S. Bouwstra and O. Leistiko: Sensors and Actuators A **52** (1996) 25.
6 A. V. Churenkov: Sensors and Actuators A **57** (1996) 21.
7 A. Ito: Optical Alliance (1997.7) p. 35.
8 V. Russo, Giancarlo C, S. Sottini and S. Trigari: Alta Frequenza **LII** (1983) 197.
9 D. Kato: J. Appl. Phys. **44** (1973) 2756.
10 M. Born and E. Wolf: Principles of Optics (Pergamon Press, 1970) p. 158.

***Katsuhisa Toshima*** graduated from Tohoku-Gakuin University, Tagajo, Japan, in 1995, and received his M.E. in electrical engineering from the same university. He is now a graduate student at the same university, and is a member of the Japan Society of Applied Physics.

***Mitsuteru Kimura*** graduated from the University of Electrocommunications, Tokyo, Japan, in 1967, and received M.E. and Dr. Eng. degrees in electronic engineering from Tohoku University, Sendai, Japan. His dissertation work addressed tunneling spectroscopy in tunneling devices. In 1974, he joined the Faculty of Engineering of Tohoku-Gakuin University, Tagajo, Japan and is presently a professor in the Department of Electrical Engineering, engaged in research on semiconductor, optical and sensor devices. He is a member of IEEE, IEICE Japan, the Japan Society of Applied Physics and the Magnetic Society of Japan.